

Morphology and tensile strength of PA6 modified PET/PP extrudates

ANGIE K. L. CHENG, W. L. CHEUNG

Department of Mechanical Engineering, The University of Hong Kong, Pokfulam Road, Hong Kong, People's Republic of China
E-mail: wlcheung@hkucc.hku.hk

Conventional fibers are straight and have generally smooth surfaces. These characteristics are not favorable for bridging matrix cracks and increasing fracture toughness during fiber pull-out. Recently, bone-shaped short fibers and end-impacted fibers have been shown to bridge matrix cracks more effectively and consume more energy during fiber pull-out [1–3]. In our study on the interfacial properties of a PET/PP (20/80) microfibrillar composite, when some PA6 (5–10%) was added to the blend during melt extrusion, a composite fiber morphology was observed. This letter depicts the morphology of the PET/PA6 composite fibers and briefly discusses the tensile properties of the extrudates.

The isotactic PP, PET and PA6 resins used were Shell VM 6100, Arnite D04 300 and Bayer Durethan B30S respectively. The blending process was carried out in a Prism 16 TC corotating twin-screw extruder. The screws had a diameter of 16 mm and an *L/D* ratio of 25. The resins were dried in an air circulation oven and then manually mixed to the predetermined weight ratios. The blends were extruded through a cap-

illary die of diameter 2 mm and then quenched in a water bath at room temperature. The extrusion parameters were similar to those for the PET/PP(20/80) blend reported elsewhere [4]. The morphologies of the extrudates were studied with a Cambridge 400 scanning electron microscope (SEM). The extrudates were cryogenically fractured and the fracture surfaces sputtered with gold-palladium before examination. Studies of the PET/PP, PET/PA6 and PP/PA6 interfaces were carried out using RuO₄ staining and transmission electron microscopy (TEM). The RuO₄ staining and ultrathin TEM sample preparation methods have been reported earlier [5]. Tensile tests of the extrudates were performed on a Lloyds 50 K tensile machine at a cross head speed of 10 mm/min. The gauge length was 10 mm and the cross-sectional areas of the extrudates were calculated based on their weights, lengths and densities. Five samples were tested for each blend.

The morphology of the PET/PP(20/80) extrudate has been reported earlier [4]. The PET fibers are generally clean and smooth, and the PET/PP interface is weak due to the incompatibility of the polymers. Fig. 1 shows

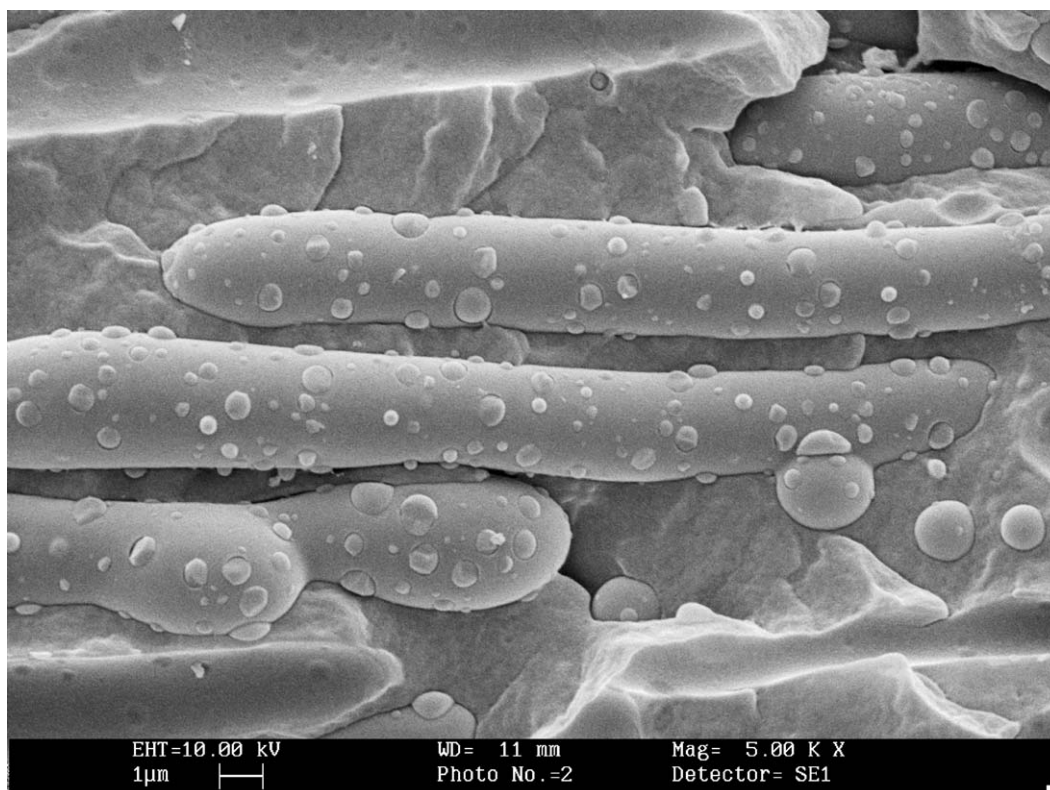


Figure 1 SEM micrograph of a longitudinal section of the PET/PA6/PP(20/5/80) extrudate.

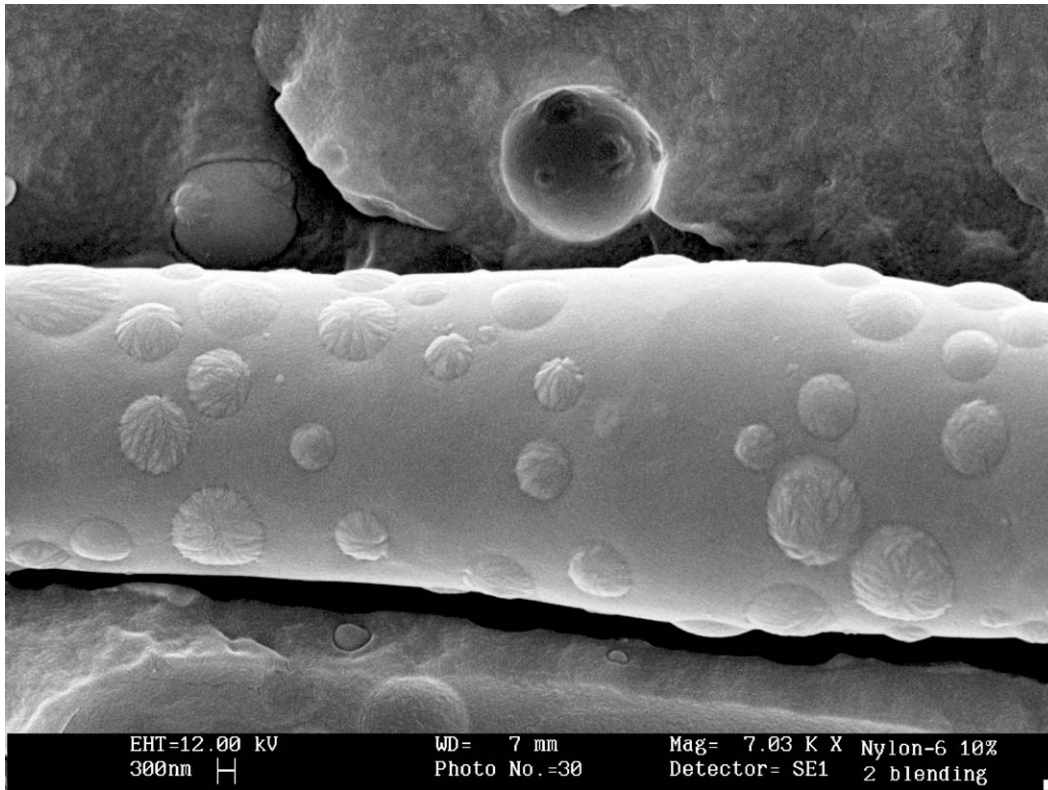


Figure 2 SEM micrograph showing a composite PET/PA6 fiber in the PET/PA6/PP (20/10/80) extrudate.

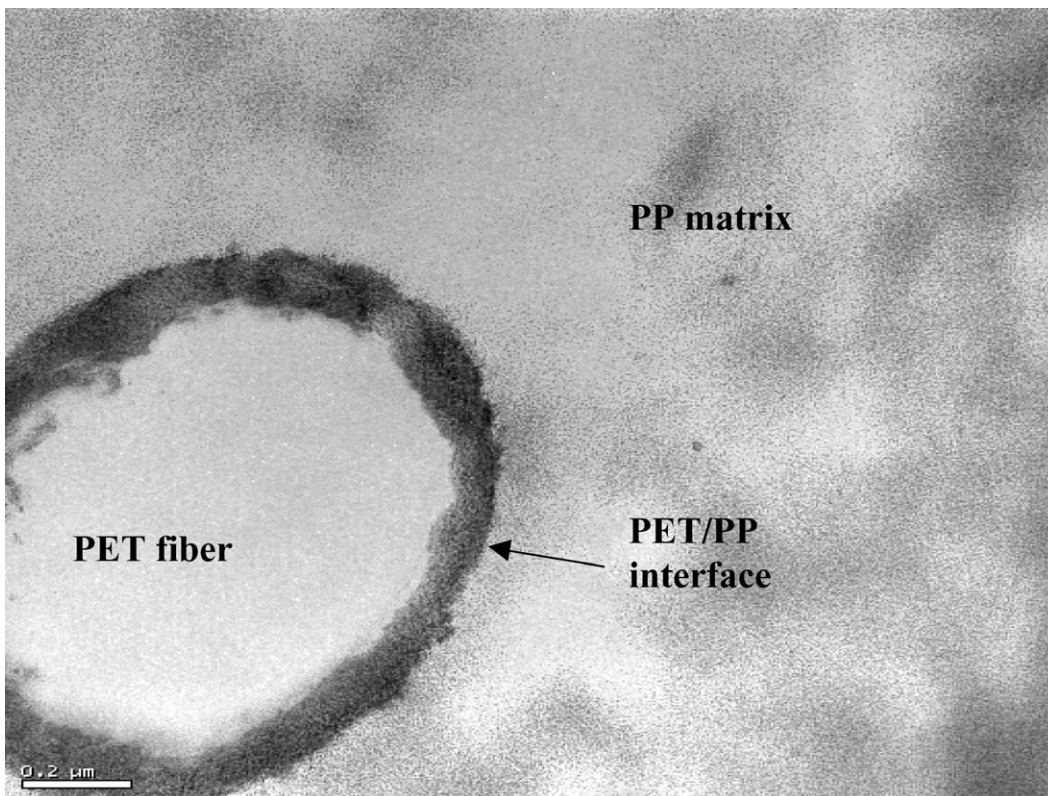


Figure 3 TEM micrograph of an ultrathin cross-section of the PET/PP(20/80) extrudate, the sample was stained with RuO₄ before sectioning.

a longitudinal section of the PET/PA6/PP(20/5/80) extrudate. Small particles are found on the PET fibers. By comparing the morphology with that of the binary PET/PP blend, it is obvious that these particles are PA6 domains partially embedded in the PET fibers. Fig. 2 shows a composite PET/PA6 fiber in the

PET/PA6/PP(20/10/80) extrudate. The PA6 domains exhibit a rough surface, which is probably a result of lamellar growth of the crystalline polymer. From an overall examination, most PA6 domains were found embedded in the PET phase and very few were present separately in the PP matrix. The affinity between

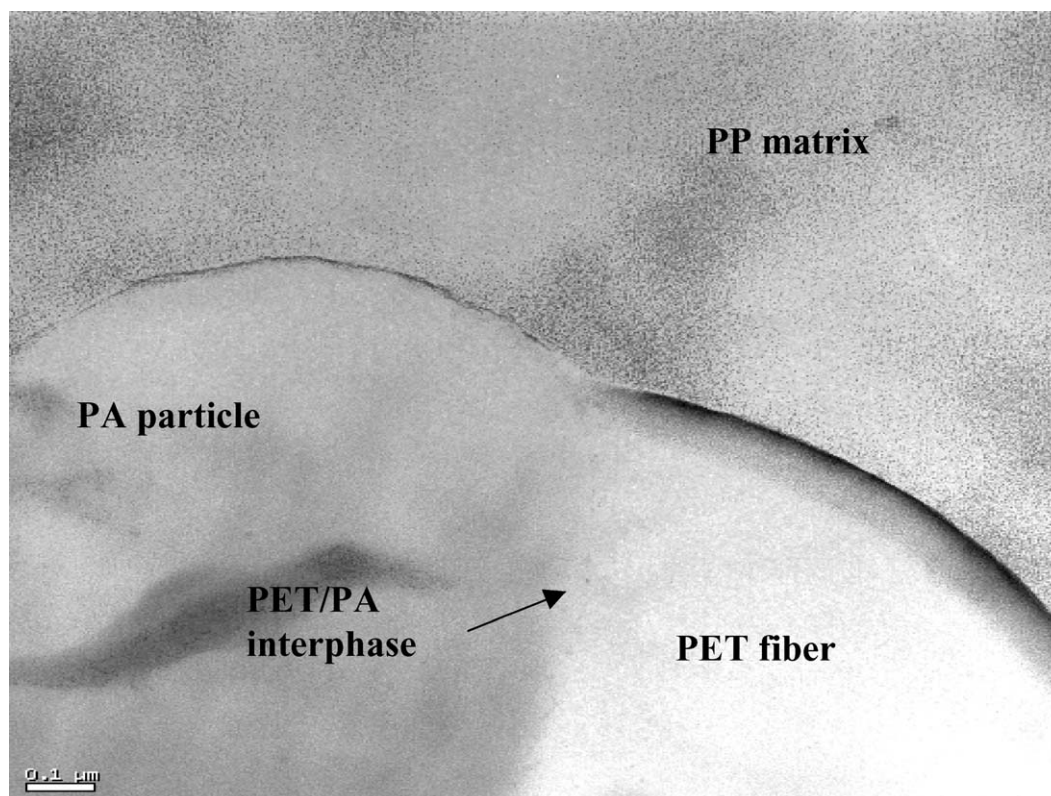


Figure 4 TEM micrograph of an ultrathin cross-section of the PET/PA6/PP(20/10/80) extrudate.

PA and PET was probably caused by copolymerisation of the two polymers during the blending process [6–7].

Fig. 3 shows a TEM micrograph of an ultrathin cross-section of the PET/PP(20/80) extrudate. The perimeter of the PET fiber was heavily stained. The phenomenon is partly due to the noncoherent PET/PP interface and partly to the highly amorphous structure of the PET fiber that facilitates diffusion of the staining agent. Fig. 4 shows an ultrathin cross-section of the PET/PA6/PP(20/10/80) extrudate. The staining effects of the three different interfaces, i.e., PET/PP, PA6/PP and PET/PA6, are different. As discussed above, the PET/PP interface is heavily stained. The PA/PP interface is also easily seen after staining, nevertheless, the width of the stained region is much smaller than that of the PET fiber. This can be attributed to the fact that PA6 and PP are more crystalline and the staining agent cannot penetrate deeply into them. In contrast, PET and PA6 appear rather coherent and their interface cannot be clearly identified. This is probably a result of the increased compatibility caused by chemical interactions between the two polymers during the melt extrusion process.

The PA6 domains protrude slightly from the PET fiber surface into the PP matrix. The phenomenon provides a mechanical interlocking effect between the fibers and the matrix, and most likely increases the interfacial friction and tensile strength of the composite. The tensile yield strength of the PET/PA6/PP(20/5/80) extrudate is about 17% higher than that of the PET/PP(20/80) extrudate, Table I. However, further increase in PA6 content causes the tensile yield strength to drop. This is probably due to a reduction in the effective cross section of the PET fibers when a large number of partially embedded PA6 particles are present.

Fig. 5 shows that the PA6 particles were still partially bonded on the PET fibers after cold drawing. Although signs of tearing are apparent in some areas of the PET/PA6 interface (arrows), the PA6 particles remain generally undeformed. This suggests that the extent of chemical interactions between the polymers is not very large and the interfacial strength is lower than the strength of the bulk polymers. It has been reported that intensive ester-amide interchange interactions take place between the polymers when *p*-toluenesulfonic acid is used as catalyst [8] or during annealing of PET/PA6 blends at elevated temperature [9]. The interfacial properties of the PET/PA6 composite fibers are expected to improve after subsequent injection molding at a temperature between the melting points of PP and PET. Furthermore, the degree of crystallinity of the PET fibers will increase after the injection molding process. These will affect the deformation characteristics of the composite fibers and hence the overall properties of the blend. The details are now under investigation.

TABLE I Tensile yield strengths of the blends

Blend	Tensile yield strength (MPa)
PET/PP(20/80)	24.5 ± 0.4
PET/PA6/PP(20/5/80)	28.6 ± 0.5
PET/PA6/PP(20/7/80)	27.5 ± 0.7
PET/PA6/PP(20/10/80)	26.7 ± 0.9

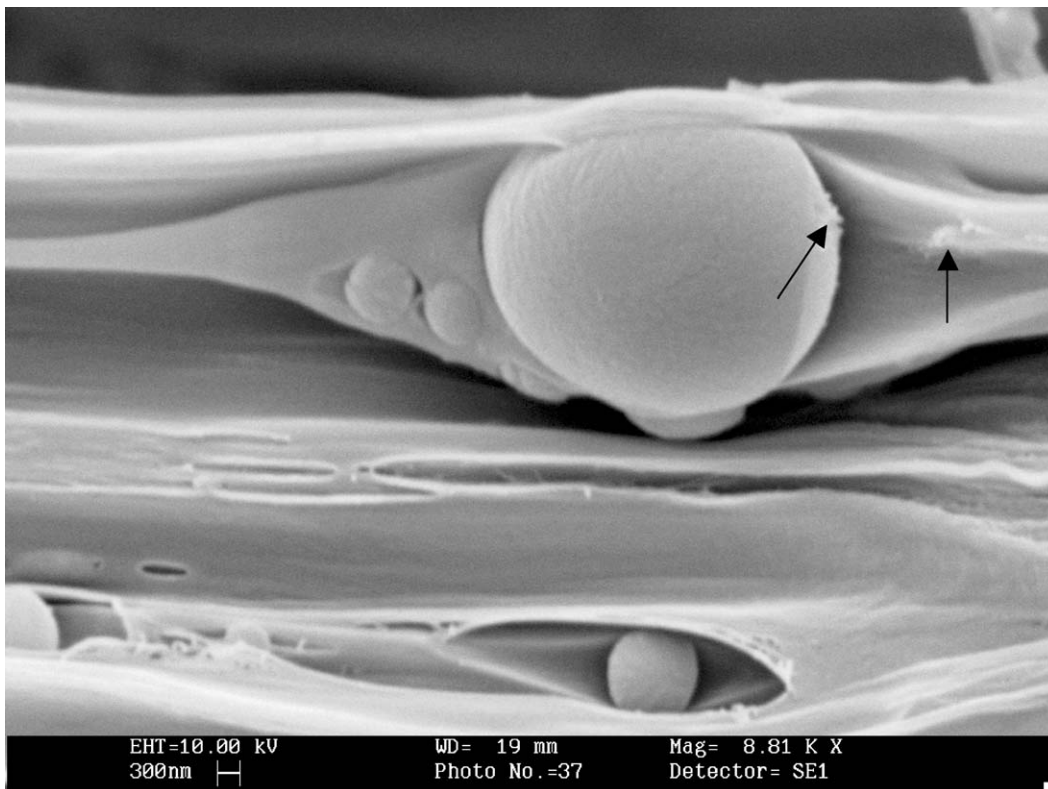


Figure 5 SEM micrograph showing a partially debonded PA6 particle on a PET fiber of the cold drawn PET/PA6/PP(20/10/80) extrudate; arrows indicate signs of tearing at the interface.

Acknowledgment

This work was supported by a CERG grant (HKU 7064/00E) of the Hong Kong Research Grants Council.

References

1. Y. T. ZHU, J. A. VALDEZ, I. J. BEYERLEIN, S. J. ZHOU, C. LIU, M. G. STOUT, D. P. BUTT and T. C. LOWE, *Acta Mater.* **47** (1999) 1767.
2. I. J. BEYERLEIN, Y. T. ZHU and S. MAHESH, *Comp. Sci. Techn.* **61** (2001) 1341.
3. R. C. WETHERHOLD and F. K. LEE, *ibid.* **61** (2001) 517.
4. X. D. LIN and W. L. CHEUNG, *J. Appl. Polym. Sci.* **88** (2003) 3100.
5. J. X. LI and W. L. CHEUNG, *ibid.* **72** (1999) 1529.
6. L. Z. PILLON, J. LARA J and D. W. PILLON, *Polym. Eng. Sci.* **27** (1987) 984.
7. S. FAVKIROV and M. EVSTATIEV, *Adv. Mater.* **6** (1994) 395.
8. L. Z. PILLON and L. A. UTRACKI, *Polym. Eng. Sci.* **24** (1984) 1300.
9. M. KRUMOVA, S. FAVKIROV, F. J. BALTA CALLEJA and M. J. EVSTATIEV, *J. Mater. Sci.* **33** (1998) 2857.

Received 14 April
and accepted 5 May 2004